SOME CONSIDERATIONS FOR A LUNAR BASED SURVEILLANCE SYSTEM

61 SPC-10

SPACE SYSTEMS

DEFENSE SYSTEMS DEPARTMENT • SANTA BARBARA, CALIFORNIA

SOME CONSIDERATIONS FOR A LUNAR BASED SURVEILLANCE SYSTEM

R. H. Brody

61 SPC-10

28 February 1962

SPACE SYSTEMS OPERATION
Defense Systems Department
GENERAL ELECTRIC COMPANY
735 State Street (P.O. Drawer QQ)
Santa Barbara, California

DISTRIBUTION LIST

Technical Libraries

Data Center - Schenectady, N. Y., (2) & 6 Cover Sheets
I & GPS, Syracuse, N. Y. (2)
TEMPO, Santa Barbara
LMED, Ithica, New York
LMED, Utica, New York
APED, Palo Alto
Elec. Lab., Syracuse, N. Y.
HMED, Court St., Syracuse, N. Y.
Comm. Products, Lynchburg, Va.
MSVD, Philadelphia, Pa.
LMED, Schenectady, N. Y.
AATD, Aircraft Accessory Turbine Dept.

DSD - Syracuse, New York

L. M. Barker
J. R. Burton
R. E. Hansen
H. Lehmann
F. E. Louther
J. G. McJilton
E. B. Mullen
R. E. Wengert
C. R. Woods

Santa Barbara, California

R. H. Brody
G. L. Dunn
L. M. Hughes
M. E. Myton
B. G. Walker

HMED, Syracuse, N. Y.

W. B. Adams
H. J. Van Ness

DA Panel, Syracuse, New York

W. T. Chapin
H. T. Clark
R. S. Grisetti
G. C. Jeffery
V. J. Louden
C. H. Pendell
S. S. Sproul

District Offices

Lexington, Mass. (2)
Huntsville, Ala. (2)
Dayton, Ohio (2)
Los Angeles, Calif. (2)
Washington, D. C. (2)

LMED, Utica, New York

S. Matt
H. Pease
A. Roeder

TABLE OF CONTENTS

LIST OF ILLUSTRATIONS

INTRODUCTION

This report covers some factors that enter into the design of a television surveillance system for a lunar mobile vehicle. The first part is a review of illumination characteristics of the lunar surface in an attempt to define the scene parameters. The second part discusses the selection of a suitable pickup tube. The final portion presents some possible system configurations. Problems involved in lunar night operation are emphasized.

SECTION I
SYSTEM REQUIREMENTS

This report presents the results of a recently completed study of factors which should be considered in the design of a lunar based surveillance system. Of primary concern is equipment for use aboard an unmanned, mobile, lunar surface vehicle. Two primary functions will be required: measurements and observations of scientific value, aids to vehicle navigation and guidance. Under the heading of the first function, one would include examination and identification of the structure and materials on the lunar surface. Also included would be monitoring of scientific experiments such as a drilling operation. For the second function, as accurate a representation as possible of the lunar surface must be presented for "steering" the vehicle across the lurrain. Stereo camera systems for range information will not be considered here as such. The main emphasis will be placed on obtaining a single clear picture. Range information in any case will be obtained from electronic processing of pictures and is beyond the scope of interest of this study.

To illustrate the value of a good clear picture, the following sequence of photographs is shown. Initially, three pictures were taken* of geological formations on earth considered to be representative of lunar surface features. These three pictures were processed through a vidicon and image orthicon closed circuit camera chain and photographed on the monitor screen as picture resolution was varied.

The first pictures (Figs. 1, 2, 3) were taken with a quality 35 mm camera and represent essentially what the eye would see. Then these pictures were processed through a closed link TV system utilizing a good quality vidicon camera. The monitor screen was photographed and the pictures are shown in Figs. 4, 5, 6. A standard 525 line, 30 frames per second, 8 megacycle bandwidth TV system was used. The scenes are clearly recognizable and competent geological opinion has indicated that lunar pictures of such quality would be useful. Next, pictures shown in Figs. 1, 2, 3 were

*These pictures were taken by F. E. Bronner, Geologist, TEMPO, who suggested this pictorial representation.

(2 1/4 x 3 1/4 Speed Graphic Photography Retouched to Simulate Lunar Conditions. Originals Taken by Finn Bronner, TEMPO, DSD)

Figure 1. Amboy Crater, California, Simulating Small Cone on Floor of Large Crater, Such as Alphonsus.

Figure 2. Front of Lava Flow Near Amboy, California, Simulating Possible Appearance of Some Inner Crater Walls.

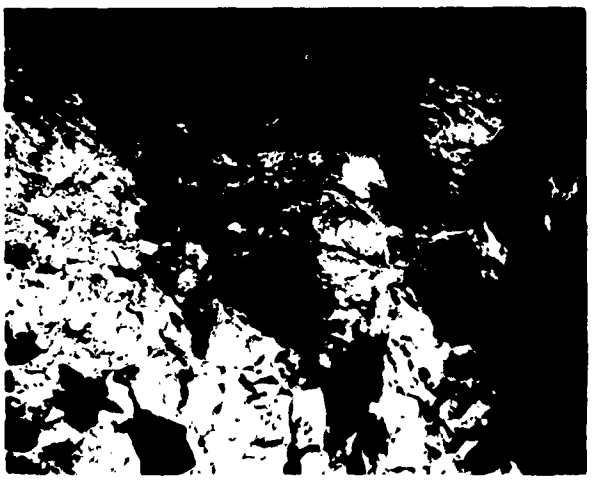

Figure 3. Crack in Lava Near Amboy, California, Simulating Possible Appearance of Lunar Cleft.

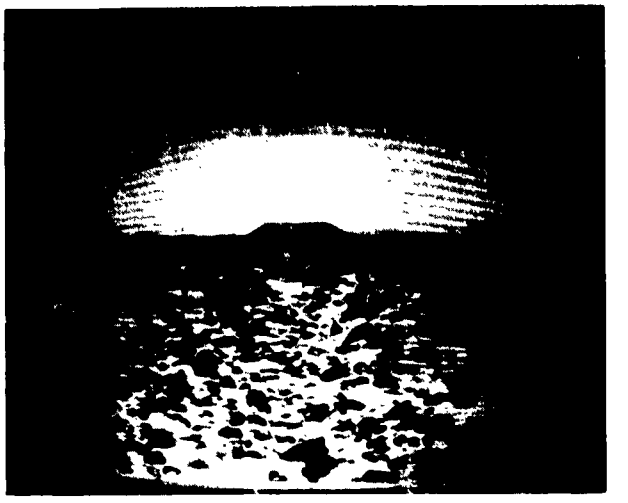

Figure 4. Photograph of a Monitor Screen Showing Vidicon Camera Presentation of Figure 1.

Figure 5. Photograph of a Monitor Screen Showing Vidicon Camera Presentation of Figure 2

Figure 6. Photograph of a Monitor Screen Showing Vidicon Camera Presentation of Figure 3

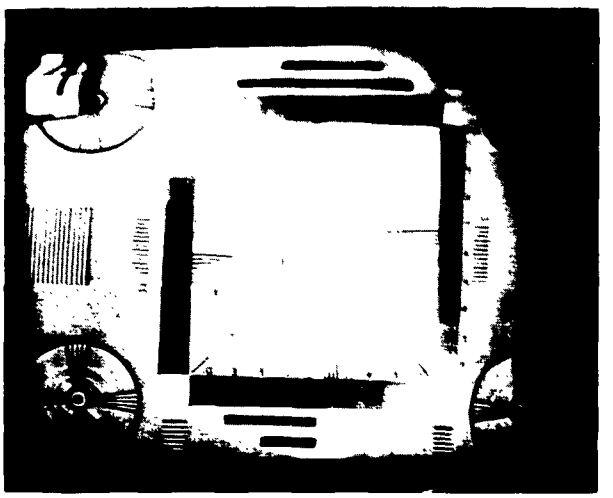

Figure 7. Test Pattern Transmitted by Image Orthicon Camera Indicating Resolution Obtained for Figures 8 and 9

Figure 8. Photograph of a Monitor Screen Showing Image Orthicon Camera Presentation of Figure 1

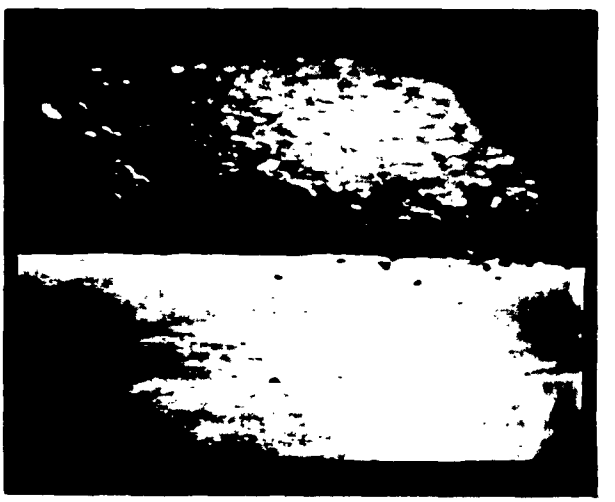

Figure 9. Photograph of a Monitor Screen Showing Image Orthicon Camera Presentation of Figure 2

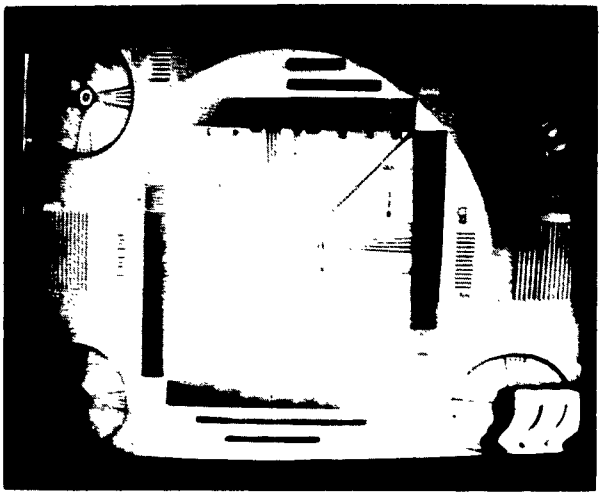

Figure 10. Test Pattern Transmitted by Image Orthicon Camera Indicating Resolution Obtained for Figures 11 and 12

Figure 11. Photograph of a Monitor Screen Showing Image Orthicon Camera Presentation of Figure 1

Figure 12. Photograph of a Monitor Screen Showing Image Orthicon Camera Presentation of Figure 2

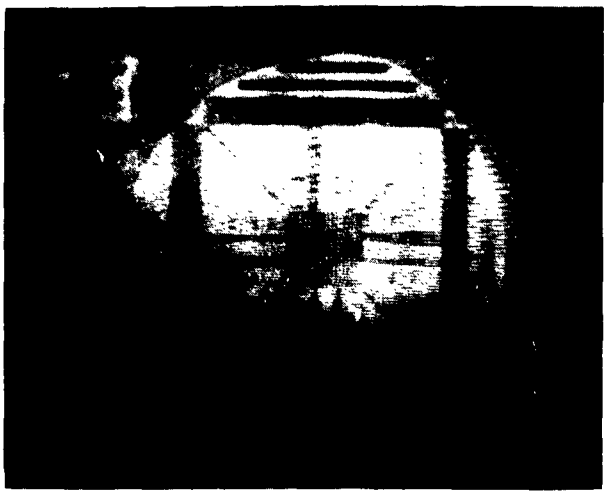

Figure 13. Test Pattern Transmitted by Image Orthicon Camera Indicating Resolution Obtained for Figures 14 and 15

Figure 14. Photograph of a Monitor Screen Showing Image Orthicon Camera Presentation of Figure 1

Figure 15. Photograph of a Monitor Screen Showing Image Orthicon Camera Presentation of Figure 2

processed through an image orthicon camera chain and the monitor display photographed. This is shown in Figs. 7 through 15. The camera aperture was varied to reduce the photo cathode illumination and effectively decrease resolution. Test patterns were photographed at each f/stop setting. These clearly show the progressive deterioration in number of effective TV lines. When one remembers that the lunar pictures must be transmitted 250, 000 miles at minimum power level, it can be seen how quickly the lunar information could become useless. Figs. 7, 8, 9 are photographs of the monitor with image orthicon stop setting at f/4. Note that the test pattern has replaced the previous picture shown in Fig. 3. Figs. 7 through 9 represent approximately a 500 line picture. Then Figs. 10 through 12 represent a 350 to 400 line picture taken at f/11. Recognition of surface features is now difficult and it can be imagined how difficult navigation of a lunar vehicle would be if this quality of picture were the only available. Finally, Figs. 13 through 15 taken at f/16 show a 250 line picture that is for all practical purposes useless.

SECTION II
SCENE CHARACTERISTICS

The following description of the luminous characteristics of the lunar surface is at best disputable. Few subjects have yielded as many interpretations of measured data as the moon. But one must have a model of the lunar surface to be able to compute scene brightness and photo cathode illumination. Consider then the following lunar data.

The brightness of the full moon is given as -10 magnitudes. The maria are only about 75% as bright as the continents. At any phase of the moon, for a fixed illumination angle, the crater rays are brighter than the continents, and the continents are brighter than the maria. Crater walls are generally brighter than crater bottoms but in very large craters, the brightness of the bottom approaches that of the walls. For the average crater there is a tendency for the brightness of the floor to decrease as the crater size increases and there is a similar relationship for the crater walls.

The albedo of the moon is defined as the ratio of the total amount of radiative energy reflected in all directions to the total amount of radiant energy incident. Measured values are: visual albedo, 7.3%; photographic albedo, 5.4%; radiometric albedo, 10%. On the average the lunar surface does not reflect more than 10% of the incident light. The individual rocks on the surface may well be a better reflector than this 10% figure indicates if the surface is rough with consequent loss of energy by scattering and absorption. Some specific regions (Ref. 1) have measured albedos as high as 30-40%. The accepted value of the albedo of average areas on the continents is 7.3% and of the maria is 4.8%.

The presence of colors on the lunar surface has been clearly established. The colors are difficult to see with the naked eye but color differences, most marked in the maria, have been detected by the naked eye. The colors of a specific spot apparently vary with time, but there is evidence this variation might be due to shadows. The continents reflect more red light than the seas.

Absolute reflectivity of lunar rocks is generally greatest in green light but crater rays reflect equally well at all wave lengths. The overall lunar surface absorbs in the wave length band 380-390 mμ. Certain spots have shown very strong ultra-violet absorbtion, i.e., Wood's spot.

The roughness of the lunar surface is deduced from several observed phenomena. Diffuse reflection from the moon does not follow Lamberts law, $I \propto \cos r$, but is closely approximated by the Lommel-Seeleger law

$$I = \frac{\cos i}{\cos i + \cos r}$$

where i is the angle of incidence of sunlight at the point observed. The brightness variations of specific lunar objects has been studied in detail as a function of phase angle. Although conclusions vary as to shape there is consistancy in the selection of a surface roughened by numerous small craterlets with protrusions between these.

A second indication of surface roughness is given by polarization of moonlight. The maria polarize more lights than the continents. When specific small areas are considered, it is found that the proportion of light polarized depends on the albedo. For the brightest areas polarization of 5% of reflected light is observed while for the darkest areas 20% has been obs rved. For surface of a given albedo the fraction of polarized light reflected from it at a given time is independent of the position on the moon's desk. This does not hold when the point in question lies close to the terminator.

When the overall lunar surface is considered at different phases, it can be seen that the percentage of polarization is greatest at the first and last quarters. This is particularly true of the last quarter when a larger proportion of dark maria is visible. No light is polarized at full moon and very little is polarized at cresent moon.

The plane of polarization lies in the sun-moon-earth plane except for phase angles between -24° to $+24^{\circ}$. At this time, near full moon, the plane of polarization turns through 90°. The maximum proportion of polarized light is approximately 1%. The general inference usually drawn from these results is that the lunar surface has very rough detail. Comparison of lunar polarization curves with measured characteristics of terrestial specimens lead to the following conclusions for composition of the lunar surface from three authors.

Continents: Maria:	Brownish, yellow sand Porous lava	Ref. 2
Pumice, powders of transparent substances (glasses, salts marble sulphur) powdered granite or sandstone		Ref. 3
Pulverized, light absorbant materials with a structure like that of black opaque gr ules		Ref. 4

The rather nebulous condition of data interpretation can be seen from these three conclusions drawn from essentially the same starting point.

The lunar surface model selected then will have the following characteristics drawn from the data above and one other source (Ref. 5).

1. The surface will be considered rough in the sense that protuberances, cracks and crevices smaller than 10 cm will abound. The surface will be covered with a layer of fine, unconsolidated particles to a depth of several millimeters.

2. The surface will be considered smooth in the sense that grades will be low, maximum of 30°, and protub - berances larger than 10 cm will not be encountered.

3. Average reflectivity will be taken as 5% for the maria surface. Objects may be encountered which have a reflectivity that ranges up to 90%.

4. The texture of the surface is such that for areas in the maria on the order of one square mile in extent, the surface will approximate a diffuse reflector and Lambert's Law.

Some justification must be given for Item 4 above in view of the previously mentioned fact that reflection from the lunar surface tends to follow the Lommel-Seeleger Law of Diffuse Reflection rather than Lambert's. Consider Fig. 16 where both functions are plotted for comparison. The Lommel-Seeleger function is plotted for three values of angle of incidence. The Lambert function is, of course, independent of this angle . The following conclusions can be drawn from Fig. 16. When the camera viewing angle is depressed 20 to 30° from the horizontal - this corresponds to an angle of reflection of 60° to 70° - the difference in reflected radiation as predicted by the two laws is less than 20%. This holds only for sun elevation angles greater than 30°. For viewing angles increasingly more depressed from the horizon, the discrepancy between the two reflection functions increases to a maximum of a factor of 3.0 at 90°. Here the surface will reflect less radiation if it obeys the Lommel-Seeleger Law. For viewing angles that vary from approximately -30° to horizontal the situation is reversed, and the surface that obeys the Lommel-Seeleger Law will reflect more strongly. At a viewing angle of 15° the discrepancy is a factor of 4.0. The comments above have assumed a flat, featureless lunar plain. Larger objects nearby, mountains or steep grades will complicate the situation.

The Lambert Law was chosen then for several reasons. First it predicts a more conservative value for the most likely range of viewing angles - from horizontal to approximately -30°. Secondly, the following analysis can be presented in a more simple form, independant of an additional dependancy on sun elevation angle. The conversion from one reflection law to the other can always be made by reference to Fig. 16 should that be desired. Thirdly, extrapolation to small area behavior directly from phenomena observed over very large areas is perhaps dangerous. There is no real assurance that areas much smaller than 1 km square follow the same reflection law as whole continents.

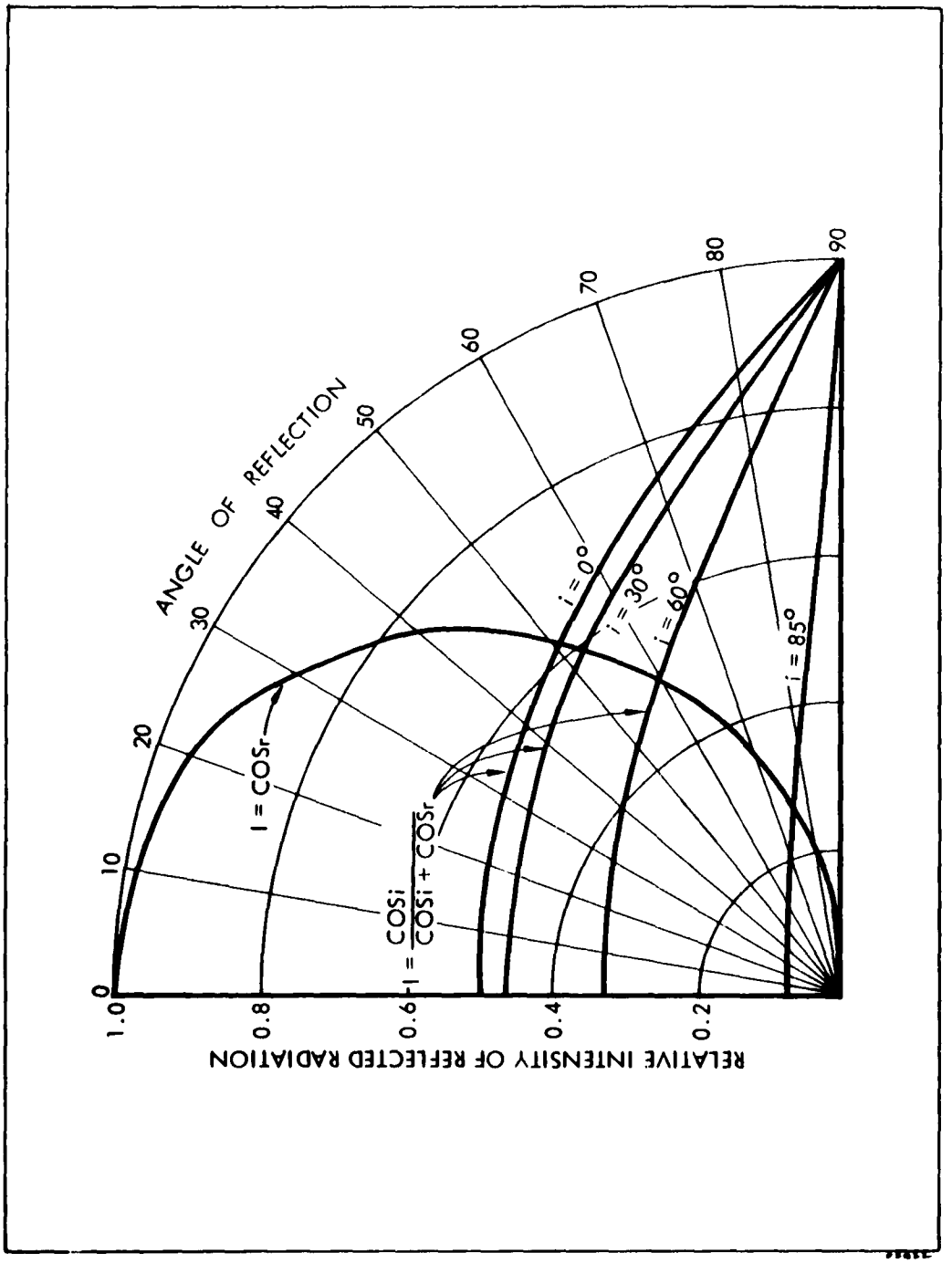

Figure 16. Radiation Reflected from a Plane Surface as a Function of Angle of Reflection Plotted for Different Laws of Diffuse Reflection: Lambert's Law and the Law of Lommel - Seeliger

The brightness of a Lambert surface is independent of viewing angle since

$$B = \frac{I\theta}{\Delta A \cos\theta}$$

where

$I\theta$ = intensity on a direction making an angle with the normal to the surface A

In = intensity along the normal

and $$B = \frac{In \cos\theta}{\Delta A \cos\theta} = \frac{In}{\Delta A} = \text{constant}$$

But the brightness of Lommel-Seeleger surface is

$$B = \frac{In \cos i}{\Delta A (\cos i + \cos\theta)\cos\theta}$$

In cases where the viewing angle warrants the conversion, Fig. 16 can be employed in a simple, straightforward manner.

Consider the illumination incident on the lunar surface now. The three main sources of illumination are the sun, earth and stars. Sunlight needs no detailed comment. Earth light or earthshine is that sunlight reflected from the earth which falls on the moon. Starlight includes all objects seen generally in the night sky such as Milky Way and planets.

Daytime lunar surface illumination is, of course, produced by the sun. A basic 27.3 day cycle results from the motion of the moon in its orbit. Nominally 13.6 days will be dark and 13.6 days will show an illumination function that increases initially, peaks and then falls off in a fashion exactly analogous to earth day and night. This behavior is illustrated in Fig. 17. Here the illumination on the lunar surface is shown as incident on three different grades. Note that the point chosen on the lunar surface is the noon sub-solar point. The grades are taken to run east-west, and have values of $+30^{\circ}$, zero, and -30°. If some point other than the

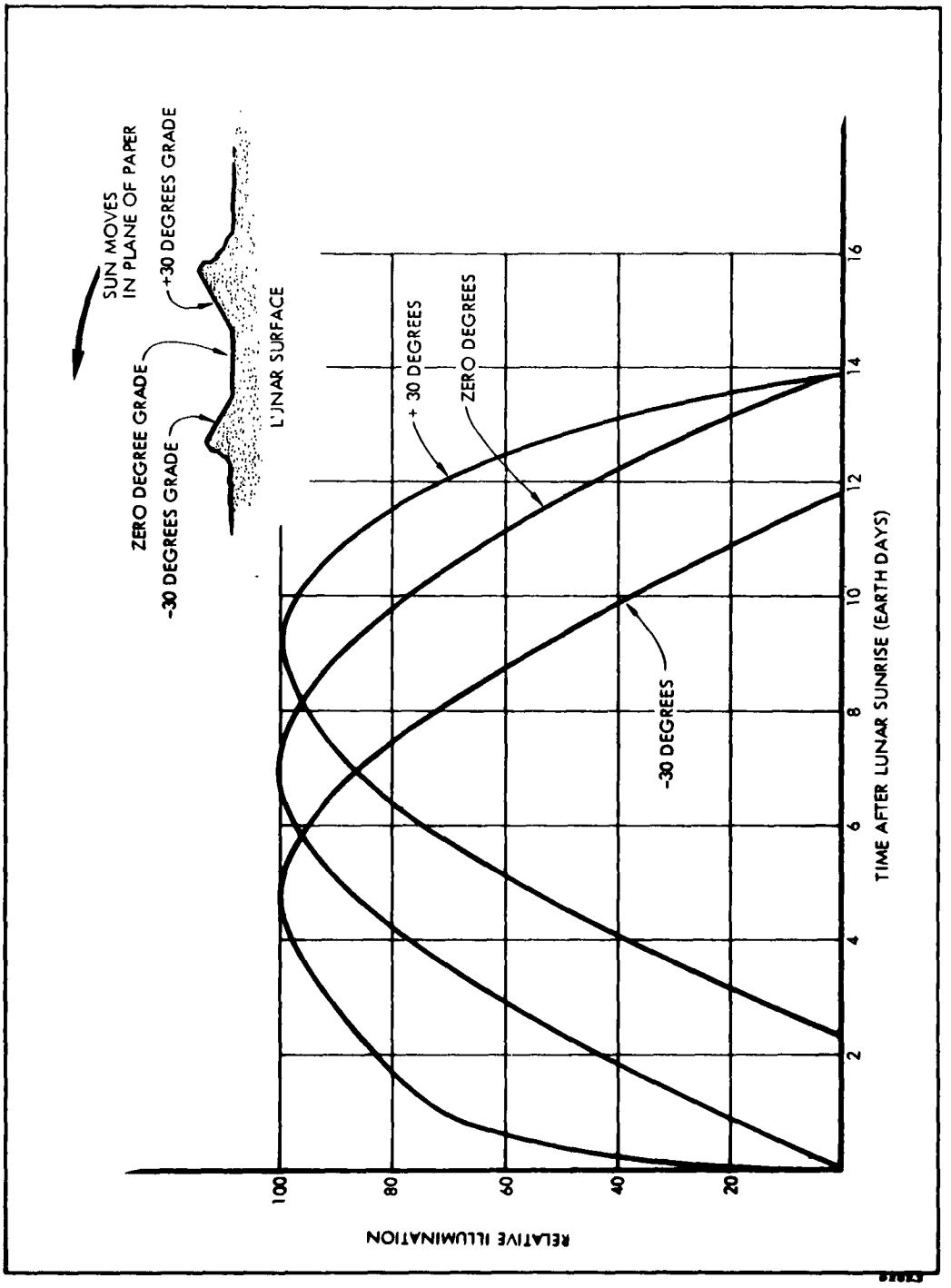

Figure 17. Variation in Lunar Surface Illumination as a Function of Time During Lunar Day

lunar noon sub-solar point is chosen, the dependence of surface illumination on lunar latitude and longitude must be considered. See Fig. 18 for earth-moon geometry used in this discussion. The lunar orbit plane precesses about the moon with an 18 year period. The exact relationship between moon, earth and sun then is a function of this precession and the position of the earth in its orbit about the sun. The sub-solar point then is lunar longitude 0 and lunar latitude 11° 31' 43" south. As the point of interest on the surface moves either north or south in latitude from 11° 31' 43" south, a modifying factor must be taken into account. To obtain the lunar surface illumination an additional multiplicative factor, equal to the cosine of the lunar central angle between the vertical and the sun must be included.

As an example, suppose it is desired to calculate the lunar surface illumination at lunar latitude 48° 21' 17" north and longitude 0 (See Fig. 19). The results plotted in Fig. 17 are valid if multiplied by cos 60° = .5. The 60° angle is that lunar central angle between latitude 11° 48' 43" south and 48° 21' 17" north. Note that no change need be made in the time axis of Fig. 17. Peak illumination will still fall at the same lunar phase. If the point of interest is considered to vary in lunar longitude, but still at latitude 11° 38' 43" south, the amplitude of illumination will remain unchanged but lunar phase will be shifted plus or minus by an angle equal to the change in longitude. If slopes oriented north-south rather than east-west had been selected initially, variations in latitude and longitude could be handled by similar simple geometric considerations.

No further discussion of this subject need be given. The reader can easily construct intensity vs. phase angle curves for any desired slope at any point on the lunar surface. It should be carefully noted that two factors which contribute to illumination on the earth do not appear here. Scattered light from the terrestial sky provides a general background of illumination incident to some degree from every direction. The moon with its tenuous atmosphere will lack this, and the result will be a serious contrast problem. To a first approximation the lunar scene may be considered to consist only of "whites" and "blacks". A second factor not considered above is light scattered from objects on the lunar surface. This scattered light will soften the contrasts

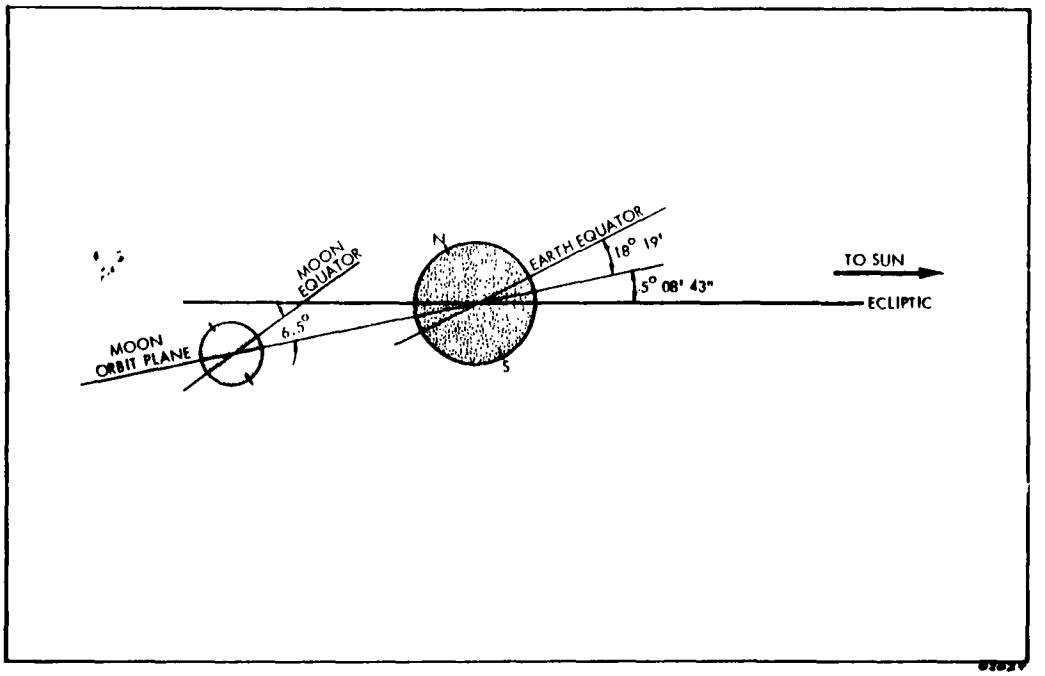

Figure 18. Relative Orientation - Moon, Earth and Eciplitic

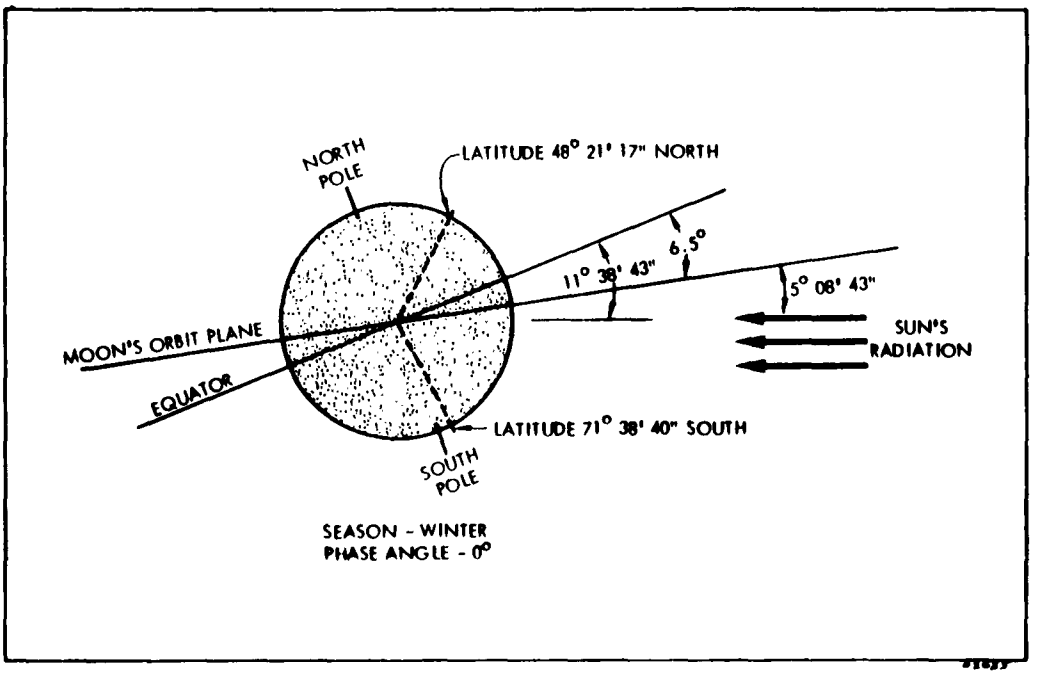

Figure 19. Geometry of Illumination of the Surface of the Moon

somewhat but not to any degree approaching that which skylight would. No attempt has been made here to account for this radiation scattered from surface to surface. A calculation of this effort requires detailed knowledge of surface optical qualities and geometry.

Consider the effect of earthshine now. The earth as a source of illumination can be significant only during the lunar night. Night time operation on the moon can be in some respects much more desirable than daytime operation. Large mobile lunar vehicles where reactor power supplies become practical are one good example where night rather than day operation may be desired. Assume 10 kw electrical power is required, and the power plant has an overall efficiency of 10%. 100 kw of thermal energy would thus be available for thermal control during the lunar night. This heat now has some practical utility where previously, during the lunar day, it posed a real disposal problem. It is then of interest to inquire as to the night time illumination level and its implication for lunar camera systems.

Fig. 20 shows the moon as it orbits about a fixed earth. The sunlight and dark sides are indicated. Three points on the side of the moon facing the earth were chosen as examples. All points are considered to be on the line defined by intersection of the earth-moon orbit plane and the moon's surface. Point 1 is at lunar longitude zero, point 2 at 45° west longitude and point 3 at 90° west longitude. Fig. 21 is derived from Fig. 20. Here one can see how the apparent phase of the earth as seen from the lunar surface varies with lunar phase angle. Note that for point 1 on the lunar surface, lunar longitude 0°, the minimum value of the earth phase never falls below half before the lunar day returns, and the surface illumination rises accordingly. For point 2, lunar longitude 45° west, lunar day returns when the illuminated portion of the earth falls to a quarter. Point 3, longitude 90° west, does not experience the return of lunar day until the cresent earth has been reduced to zero. Symmetrical plots would, of course, be obtained for points on the lunar surface from longitude 0° to 90° east. The illumination on the lunar surface due to "earthshine" will vary as the apparent phase of the earth seen from the moon and the lunar latitude and longitude. The maximum value will occur only for point 1 at a lunar phase angle of 180°.

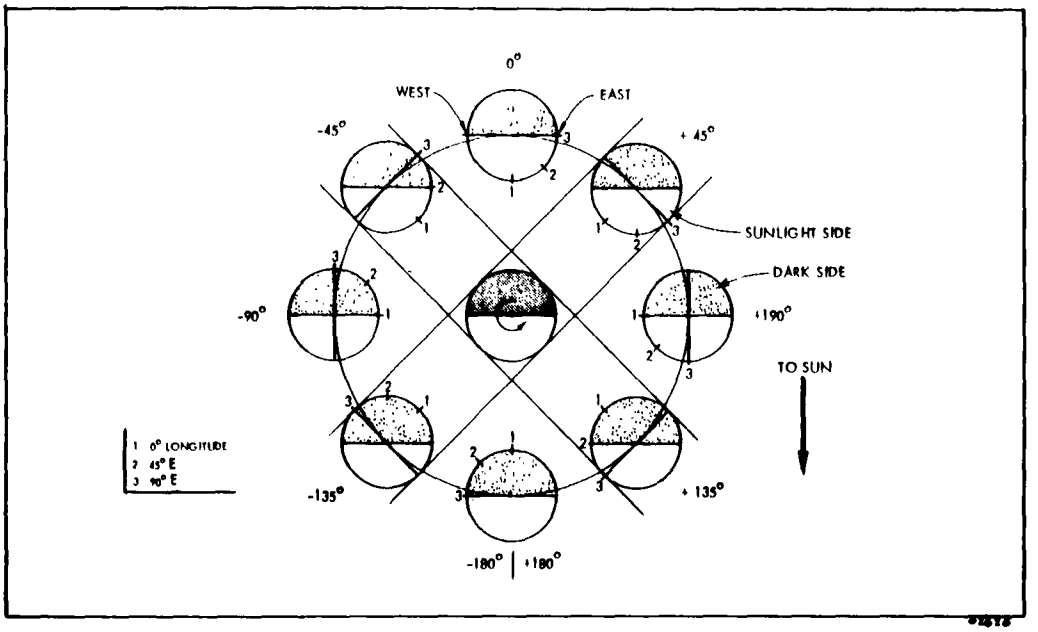

Figure 20. Earth-Moon Relationships for Determining Lunar Surface Illumination due to Earth Shine

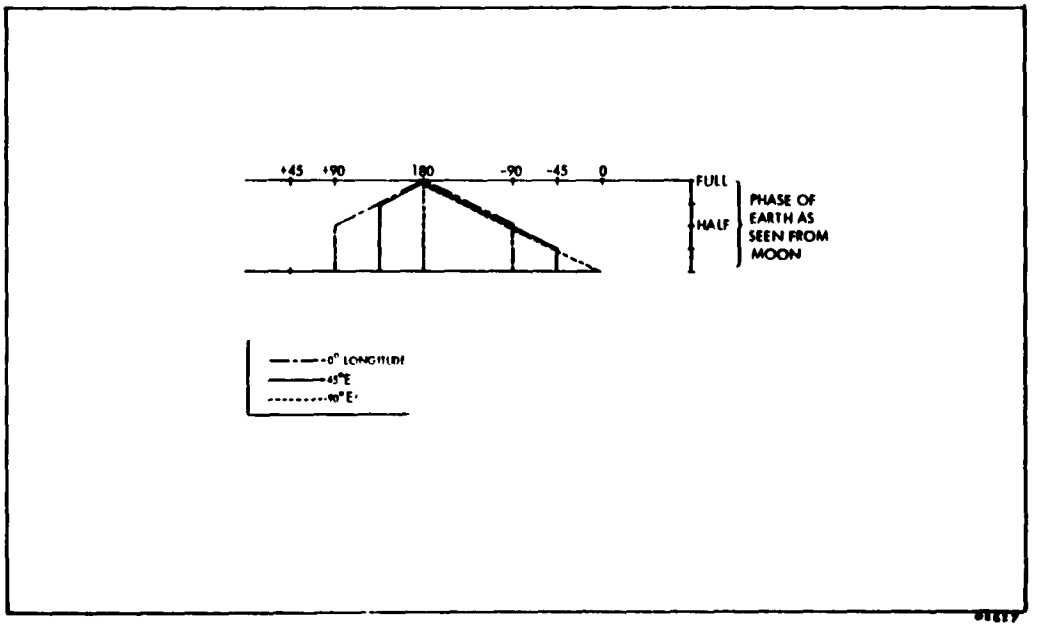

Figure 21. Phase of Earth as seen from Three Points on Lunar Surface as a Function of Lunar Phase Angle

Star light will present essentially a constant background illumination independent of rotation or orbit position. The value taken for this is 9×10^{-5} foot candles (Ref. 6).

One must now obtain the lunar surface illumination as a function of the phases of the earth. For the full earth, as seen from the moon, the calculation is straightforward. One can scale from measured data on moonlight. It is known that full moonlight on the earth produces 0.02 foot candles. The earth's albedo is 37% and the moon's 7%. The relative areas of the earth and lunar disc are in the ratio of the squares of the radius. Therefore, one can say the illumination produced by a full earth is, neglecting attenuation by the earth's atmosphere,

$$I_1 = (0.02) \times \frac{(37)}{(9)} \times \left(\frac{1.000}{.273}\right)^2 \text{ foot candles} = 1.1 \text{ foot candles}$$

Now some relationship between other phases of the earth and lunar surface illumination must be found. A curve (Ref. 7) showing the intensity of the integrated light from the moon as a function of lunar phase is given in Fig. 22. Surface illumination can be taken as directly proportional to the source intensity. If it is now assumed that the earth obeys the same reflective laws as the moon, one can use the curve in Fig. 22. This is, of course, only an approximation. For example, it will be noted that the lunar intensity curve is not symmetrical with respect to positive and negative phase. This is caused by a preponderance of high reflectance continental area on the west side of the moon as contrasted with preponderance of more on the east side. (These directions are those noted on an astronomical picture of the moon.) The earth, as it rotates with a 24 hour period, might be expected to show analogous variations in intensity from such varying reflective surfaces as continent to ocean and cloud-free area to completely overcase area. In addition to these short, 24 hour modulations of the earth's intensity, one would also expect long term modulations corresponding to seasonal changes on the earth. The actual intensity vs. phase for the earth might be quite different from that shown in Fig. 22. But until direct measurements are available, it is perhaps reasonable to use the above curve as a first approximation.

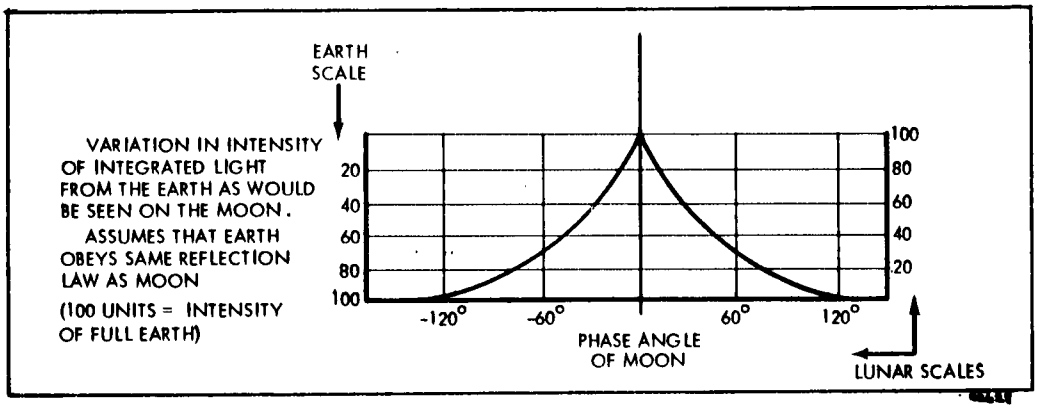

Figure 22. Variation in Intensity of Integrated Light of the Moon as Seen from Earth (100 Units = Intensity of Full Moon)

The lunar surface illumination due to earthshine is shown in Fig. 23 as a function of earth phase for the three lunar longitudes previously shown in Fig. 21. Note that for the case where lunar longitude is zero degrees, illunination never falls below 0.1 foot candle. The lunar latitude, as specified in Fig. 21 is that in the plane of the earth-moon orbit of $6^{\circ}\,30'$ south. No further use would be served in computing variations in illumination with latitude, longitude, and surface inclination. The approach would exactly parallel that given above for sunlight. It is only important to note that scene illumination can be calculated for any point on the moon. And within limits, one can prescribe some range which will cover maximum anticipated slopes. If one makes some judicious assumptions concerning surface texture and reflectivity, a range of scene brightness values can be derived to allow a system design.

Let us assume a lunar mission where impact will occur within $\pm 5^{\circ}$ of the lunar equator between 40° and 50° east longitude. This area is in the mare roughly south of the crater Kepler. The illumination level through one full lunar day and night is shown in Fig. 24 where a flat, level plain has been assumed. Note that this region will always receive either direct sunlight or earthshine. The illumination level then never falls to that of starlight alone - 9×10^{-5} foot candles. Scene brightness values for this impact point are plotted in Fig. 24 on separate scales. The average portion of the scene is assumed to have a reflectivity equal to 10%. In a later section, these values for scene brightness will be interpreted in terms of camera system parameters.

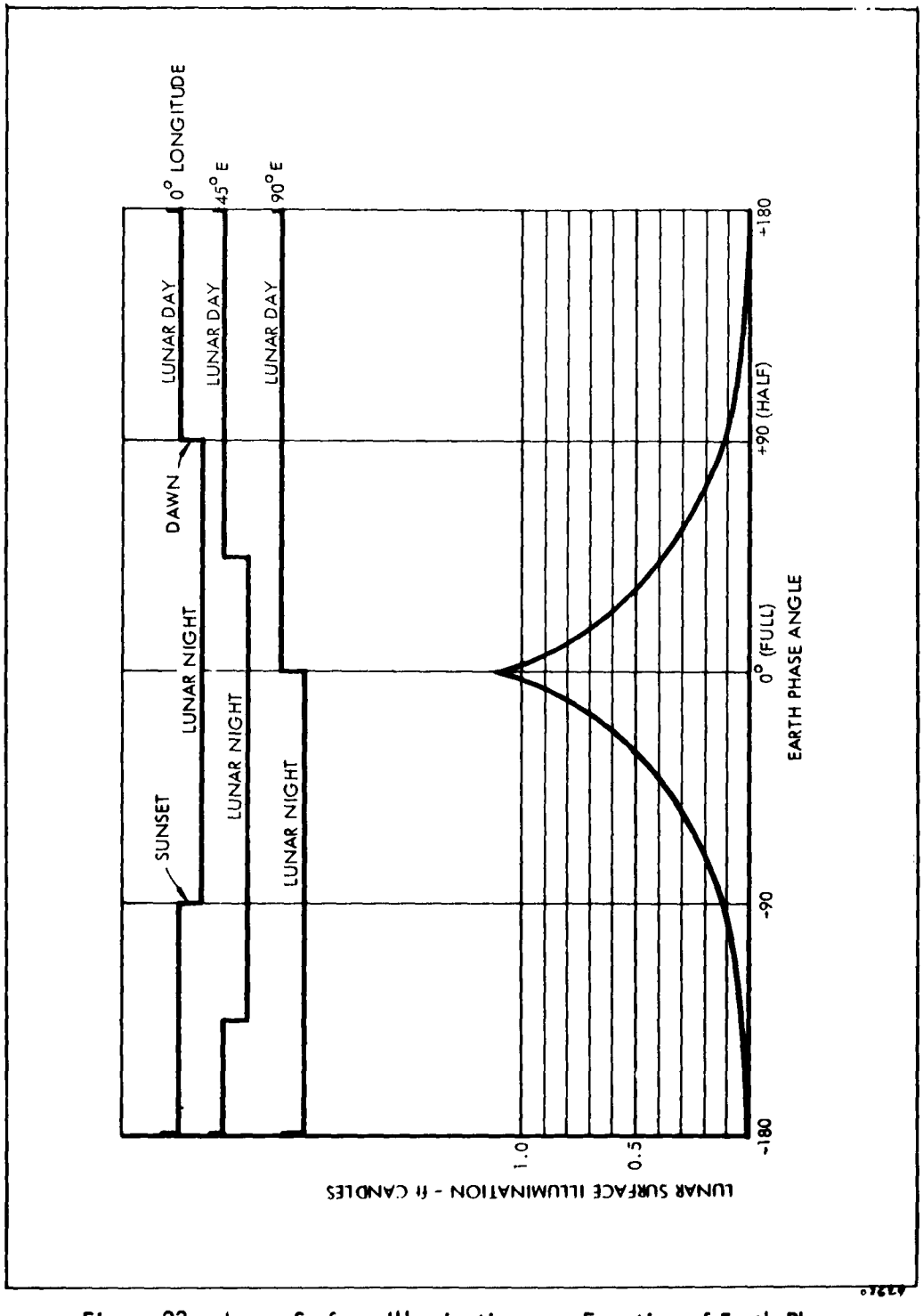

Figure 23. Lunar Surface Illumination as a Function of Earth Phase

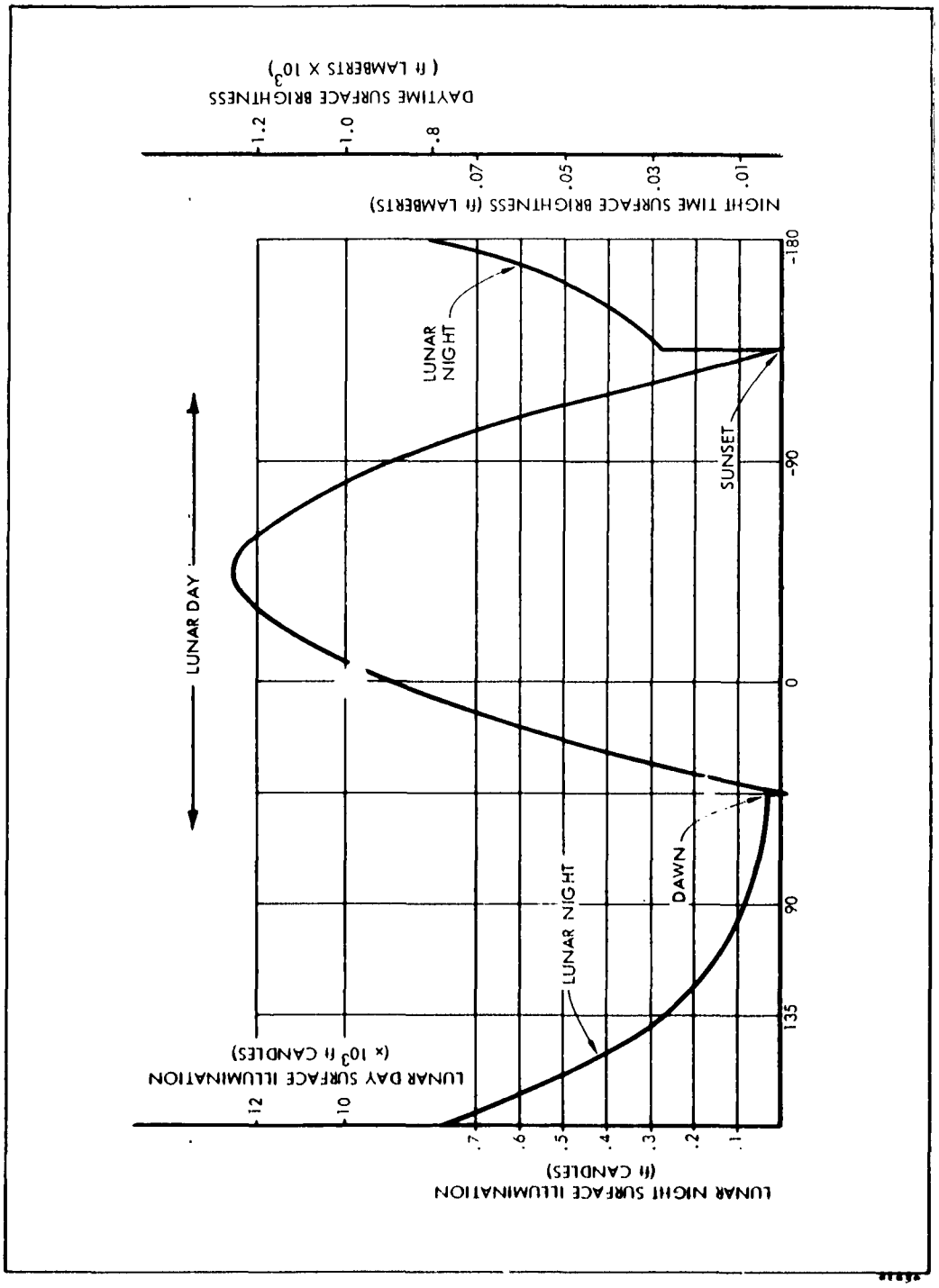

Figure 24. Lunar Surface Illumination Characteristics Plotted for One Day/Night Cycle

SECTION III
PICTURE PICKUPS

The following section describes in general terms some of the operating characteristics of three possible picture pickups - the image orthicon, the vidicon and the latent image camera.

A. Image Orthicon

The Image Orthicon is a light-sensitive television camera tube used as the transducer in the conversion of an optical image to an electronic video signal. (Fig. 25) An optical image of the scene is formed by a suitable lens system through the faceplate of the tube on to the photoemissive cathode. The light falling on the photocathode produces an electron image which is focused through a copper mesh on to a storage target surface. In conventional tubes this target is a glass membrane, two 10-thousandths of an inch thick. In high sensitivity G. E. image orthicons, the target is a very thin film of magnesium oxide.

The electrons from the photocathode in striking the target, produce a greater number of secondary electrons which are collected by the copper mesh, thus producing a positive charge pattern on the target. The standard glass target uses sodium ions to conduct the charge from one side of the target to the other. These ions conduct the positive charge (produced by emission of secondary electrons) from the photocathode side to the scanning beam side of the target where they are neutralized by the scanning beam and, in turn, modulate the beam to produce a video signal. The depletion of sodium ions in the glass target requires progressively longer periods of time to burn out the preceding scene as the tube ages. This depletion process is a factor limiting the useful life of image orthicons with glass targets.

The thin-film magnesium oxide target utilizes electron conduction rather than ion conduction. Charges are conducted from the scanning-beam side of the magnesium oxide target to the photocathode side by free electrons which are supplied by the scanning beam. Electron conduction is not a depletion process, therefore the life of a

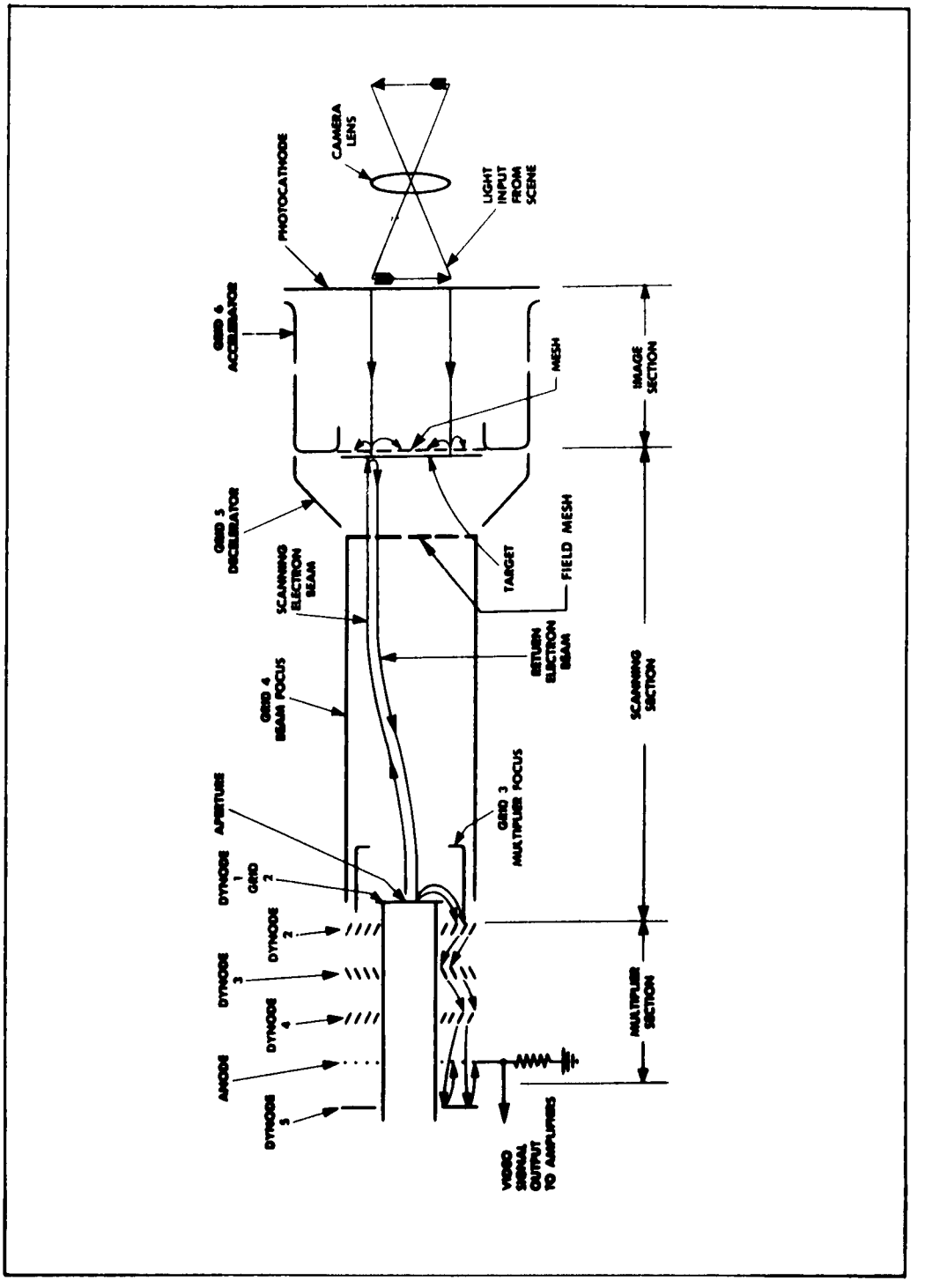

Figure 25. Image Orthicon, Functional Diagram

magnesium-oxide target image orthicon is not dependent upon the target. Some tubes in life tests have exceeded 12,000 operating hours with good sensitivity and no burn in.

The outstanding advantage in using an image orthicon is the high sensitivity. Excellent pictures can be taken in full moonlight. Satisfactory pictures are obtainable using only the illumination from a clear, star filled sky at night. Where highest possible sensitivity is an important system requirement the image orthicon is a strong contender. However, when one considers the operating limitations on the camera tube the image orthicon appears less desirable. The allowable orientations of the tube are restricted to avoid damage and the fragile target by particles within the tube. Temperature of the cathode end must be closely controlled. Set-up and adjustment of the tube for different operating conditions is complex.

B. Vidicon

The vidicon differs from the image orthicon in several important ways. First, no image intensifier is used. Secondly, no electron multipliers used to boost the signal level. The major effect of this is to assure that system noise is set by the preamp rather than the beam noise. Detection of a signal is primarily a photo conductive process. The scene is focused on a photocathode. Then this cathode is scanned by an electron beam which "discharges" each element as the beam passes. The current required to discharge each element flows through a series resistor and the preamp reads this voltage out. The most attractive feature of the vidicon compared to the Image Orthicon is its simplicity. When sensitivity is the overriding consideration, the Image Orthicon is clearly the detector to use. When simplicity, reliability, and compactness are of primary importance, the vidicon comes into its own. In general, vidicons are manufactured with magnetic deflection but units are becoming available with electrostatic deflection and focus. The savings in weight and power consumption with electrostati deflection is appreciable.

An interesting description of the camera system for Ranger (Ref. 8) is reproduced below. This article does a good job in describing general system problems and the best state-of-the-art solution.

"Vidicon System For Ranger

"The television system for Rangers RA-3, -4, and -5 has been tailored specifically for the experiment and thus departs in several areas from typical designs. A vidicon sensor was chosen for imaging because of its simplicity and ease of operation. Quite unlike other vidicon camera systems, an all-electrostatic deflection and focus vidicon is employed which combines a special 'sticky' target with rapid erase capability. In operation, an image is shuttered onto the faceplate for 20 milliseconds and the slowly decaying image is subsequently scanned at a rate which yields one complete frame in 10 seconds. Two hundred scanning lines are employed per frame in order to achieve the desired resolution. The video band-width out of such a system for equal vertical and horizontal resolution is of the order of 2000 cycles.

"Since each frame is different from the rest, no averaging technique for a large number of frames may be employed for background shading or dc restoration; thus, the lowest frequency in the video signal must be considered to approach dc. In order to accommodate this, the vidicon beam current is modulated by a high frequency which chops the target current and creates an amplitude modulated signal. After sufficient amplification, the demodulated video is mixed with blanking pulses to form a composite video signal for presentation to telemetry. The line-deflection circuit is triggered from a 20 cps generator clocked, in turn, from the spacecraft 400 cps. Since this 400-cps clock is available in the ground receiver, line synchronization is guaranteed even in the presence of rather severe noise; or, in turn, the 400-cps clock may be retrieved from the line sync pulses should the 400-cps signal be lost. The commands for shutter and erase are obtained from the CC & S in the form of 1-millisecond switch closures. The shutter command terminates erase, triggers the shutter solenoid drives and, following a fraction second delay, causes initiation of the frame sweep. The erase command terminates the frame sweep and initiates the erase mode which consists of illumination of six filamentary lamps mounted on the periphery of the vidicon target, acceleration of line and frame scan rates over the surface of the target, and increased beam current. Although this process normally requires less than 1 second, circuit simplicity is maintained by continuing erasure for the full 3 seconds allotted for readout of the gamma-ray data.

"The vidicon sensor was chosen as the result of an extensive evaluation program. All available sensors were investigated by RCA as a preliminary phase of the impact television contract. The specific requirements on the vidicon are:

1. Adequate sensitivity for low light levels anticipated.
2. Sufficient dynamic range to allow perception of detail for lower than normal illumination as well as possible strong highlight detail.
3. Capability of survival of the thermal requirements of bulk sterilization.
4. Minimum weight and power requirements.
5. Adequate storage time of a shuttered image combined with ease of erasure prior to shuttering of a new optical image.

"These requirements of the sensor were not mutually compatible in light of present commercial practices. Thus, it was evident that a completely new sensor would have to be developed which combines the best features of existing sensors and yet meets the rigors of spacecraft environment. Since this is an evolutionary development which normally requires extensive time, it is a credit to the participating organizations that a task of this nature was actually accomplished within the demands of the Ranger schedule. The resultant sensor combines all the required features.

"The target material chosen for this vidicon is an antimony sulfide oxysulfide surface which is a proprietary development of RCA and combines the necessary retention of the image for slow scan readout together with rapid erase capability. The latent image may be scanned slowly off the target with less than 10% reduction in highlight detail for periods in excess of 10 seconds. Sensitivity of the surface is maintained at light levels as low as 0.01 ft-candle-sec following the 24-hour soak at 125° C. for sterilization; the useful dynamic range of some units extends from 0.001 to 0.1 ft-candle-sec with an opening of f/6 and 20-millisecond exposure. The image may be erased in 700 milliseconds.

"The electron gun structure and deflection system is a ruggedized version of the 1-inch diameter electrostatic unit manufactured by General Electro-dynamics Corporation (GEC). Electrostatic focus is accomplished by a saddle field lens arrangement and electrostatic

deflection is accomplished through the use of special deflection plate configuration designed by Schlesinger called a Deflectron. The conventional crossed pair deflection plates cause the electron beam to be deflected sequentially; that is, in passing between the first set of plates, it is deflected in one plane, and then when reaching the second set of plates, it is deflected in the other plane. The Deflectron causes the beam to be deflected both horizontally and vertically simultaneously as in magnetic deflection. This common center of deflection reduces the undesirable effects of fringe fields, defocusing, and other distortion found in conventional plate scanning.

"Physically, the Deflectron is a tube of insulating material, the inside of which contains the printed deflection plate pattern. This yields an exceptionally rugged structure capable of surviving present spacecraft environment. In addition, the use of an all-electrostatic structure removes the considerable weight and power penalty of electromagnetic deflection yokes, while resolution comparable to electromagnetic systems is maintained through the use of post-deflection focusing.

"The faceplate complete with target material is supplied by RCA and is bonded by GEC to their gun structure by an indium-glass seal process tailored specifically for this particular vidicon. The electron gun structure has been modified to permit a larger beam diameter. This was done in order to facilitate rapid erasure of the sticky target, since erasure is accomplished by simultaneous application of external light stimulus and rapid-scan of the target in 'fire hose' fashion by the electron beam. Dark current slipping over wide temperature ranges is facilitated by including a deposited mask on the faceplate to obscure a portion of the image. This mask covers a narrow strip along the faceplate which obscures less than 5% of each scan line. Present vidicons have this mask vapor deposited externally; however, experimentation with internal deposition is in process and, if successful, will eliminate the slight amount of optical defocusing presently observed with this mask."

C. Electrostatic Latent Image Camera

This is a General Electric development sometimes suggested as a possible alternative to "conventional" - i.e., vidicon, orthicon - cameras. In the new approach, an image is found on a photo-conductive sheet, CdS, and then transferred to thermo-plastic tape. Conventional TPR techniques are then applied.

System angular resolution is determined by the process resolution and the lens focal length. A process design goal of 100 line pairs per millimeter is expected to be achieved within the near future. In the present laboratory model, a system resolution has been demonstrated of 40 line pairs per millimeter over a 60 mm square format; i.e., 2400 lines per frame. This demonstrated resolution, used with a lens of 6 inch focal length (giving a field of view of about 23° on the 60 x 60 mm film format) will yield an angular resolution of about 0.01° or 0.17 milliradians.

This system is not sufficiently developed to undergo environmental tests. However, some qualitative characteristics can be stated. In contrast to photographic film the system is expected to be very radiation resistant. Both the thermoplastic tape storage medium and the photoconducting sensor, the key elements of the system are expected to provide this tolerance. On the other hand, it appears that these elements of the system will need to be operated in a controlled atmosphere, hermetically sealed particularly against moisture or high humidity, no real problem on the moon. Also, because of the thermoplastic itself, the internal temperature must be held below 85° C. Otherwise the system could be considered environmentally much in the same category as a photographic camera with electronic readout.

The present development schedule specified delivery of a feasibility laboratory breadboard in August, 1961. About a year of additional applied research and development is needed before development of an engineering model could begin. Hence, a first prototype might reasonably be achieved some time during 1965 with an operational model available in 1966.

The latent image camera can be summarized then as containing promise but should not be considered as operational equipment for the next several years.

The choice of camera system for lunar surveillance can then be made. The utmost in reliability and simplicity is required. Estimates made of the dollar cost in placing the first Prospector on the lunar surface are of the order of 1 billion dollars. The cost for 5 Surveyor spacecrafts came to 50 million dollars. This does not include booster or launch costs. It is easily seen why JPL insists on proven concepts and equipment for lunar and planetary programs. The image orthicon has improved greatly in the last few years. The new General Electric tube with the magnesium oxide target represents a major stride forward. But the image orthicon is still a bulky, complex, and delicate instrument when compared to the vidicon. It will further be seen that the high sensitivity of the image orthicon is not required for lunar daytime operation. Image orthicons with electrostatic deflection and focus are in the talking stage but vidicons so equipped have been built. Vidicon resolution is as good or better than that of image orthicons. As noted in the JPL discussion above, new vidicons with sufficient sensitivity for limited lunar night operation are being developed for the Ranger Program.

The electrostatic latent image camera is another General Electric development of great promise. But equipment is far from being sufficiently developed to warrant serious consideration at this time.

The choice is clearly the vidicon.

SECTION IV
SURVEILLANCE SYSTEM PARAMETERS

This section of the report will present an equation relating camera system parameters—as for example, resolution, frame rate and lens diameter – to lunar scene brightness levels. The range of these parameters will then be studied for feasible system designs.

The equation relating camera parameters given below follows that of Rose (Refs 9, 10).

$$B = \frac{2.8}{\pi} \quad \frac{f^2 (s/n)^2 \; n_q \times 10^{-13}}{T \; t_1 \; a} \qquad (1)$$

where

B	=	scene brightness in foot lamberts
f	=	lens f number
T	=	lens transmission
t_1	=	frame time in seconds
a	=	elemental detector area in square centimeters
s/n	=	signal-to-noise ratio
n_q	=	number of incident photons required to produce a barely discernible photoelectric response from the photocathode.

For an ideal pickup tube n_q would be equal to unity. One incident photon produces one electron. In the case of a vidicon where the noise level is set by the preamplifier one must express n_q in terms of photocathode quantum efficiency and amplifier bandwidth.

The equivalent rms noise current of the preamplifier can be written as

$$I_n = 2 \sqrt{\frac{KT}{R} \; f_m \left(\frac{1 + R_t R \; 4 \; ^2 f_m \; ^2 C^2}{3} \right)} \qquad (2)$$

where

K = Boltzman's constant = 1.38×10^{-16} erg/°K
T = temperature in °K
R = input resistance of amplifier
f_m = bandwidth of amplifier
R_t = equivalent noise input resistance of first amplifier stage

If R is taken to be large, I_n becomes

$$I_n = 2\sqrt{\frac{KTf_m R_t (W_m C)^2}{3}} \qquad (3)$$

where

$$W_m = 2\pi f_m$$

Assume "reasonable" values for R_t and C such as

R_t = 500 ohms
C = 2.6×10^{-11} farads

Then (3) becomes

$$I_n = f_m^{3/2} \times 2.8 \times 10^{-19} \text{ amps} \qquad (4)$$

The bandwidth can be expressed as

$$f_m = \frac{N}{2t_1}$$

where

N = total number of picture elements
t_1 = exposure time per element or one frame time

And (4) becomes

$$I_n = \left(\frac{N}{t_1} \right)^{3/2} \times 10^{-19} \text{ amps} \qquad (5)$$

Return now to the threshold picture where signal current is just equal to noise current. The signal current is the total photo electron current from the photo sensitive surface. One can write the following experssion for the threshold number of electrons per picture element.

$$n_e = \frac{I_n t_1}{N Q} \qquad (6)$$

Since signal current is

$$I_s = \frac{n_e Q}{t_{ro}} = I_n$$

where:

$t_{ro} = \frac{t_1}{N}$ readout time for one picture element

Q = electron charge
= 1.6×10^{-19} coulombs/electron

Combining equations (5) and (6) one obtains

$$n_e = 0.6 \left(\frac{N}{t_1} \right)^{1/2}$$

And if the quantum yield of the photo process in $\ominus$, where $\ominus$ = number of electrons produced per incident photon, the threshold number of quanta per picture element may be written

$$n_q = n_{e/\ominus} = \frac{0.6}{\ominus} \left(\frac{N}{t_1} \right)^{1/2} \qquad (7)$$

Equation (1) then becomes

$$B = \frac{2.8}{\pi} \frac{f^2 (s/n)^2 \ 0.6}{T \ t_1 \ a \ \Theta} \sqrt{\frac{N}{t_1}} \times 10^{-13} \text{ ft lamberts} \tag{8}$$

Equation (8) can now be expressed in a more convenient form

$$B = \frac{2.8}{\pi} \frac{(s/n)^2 \sqrt{\frac{N}{t_1}}}{T D^2 \alpha^2 t_1} \frac{0.6 \times 10^{-13}}{\Theta} \text{ ft lamberts} \tag{9}$$

where

D = lens diameter in centimeters
α = elemental resolution in radians

Take an example now to illustrate the usefulness of the expression above.

Consider again the lunar landing point discussed in a preceeding section where scene brightness data was given in Figure 24. Consider day viewing first. The peak scene brightness is 12.7 x 10^2 foot lamberts. One hour after dawn and one hour before sunset, the level is approximately 60 foot lamberts. It is assumed that surface reflectivity, taken as 10%, is independent of angle of incidence. Consider now the relationship between camera system parameters for a vidicon camera designed to operate over this scene brightness range.

Assume a 500 x 500 line picture. Aspect ratio is therefore 1:1. The desired field of view will range from 5.0° square, for detailed examination of a particular area, to 50° square for general viewing and surveillance. The incremental resolution then will vary from 0.01° to 0.10° or 0.18 milliradians to 1.8 milliradians. N therefore is 2.5 x 10^5. Note that the value for α as obtained from equation (2) has no direct relationship with another measure of resolution, the field of view divided by the number of scanning lines. The value of α represents the resolution limit inherent in

the photo sensitive cathode and is determined exclusively by the number of incident light quanta. No consideration is given at this point to optical image size. Whether or not this ultimate photo cathode resolution is in fact realized in usage will depend on optics, field of view, number of scanning lines and other factors. But the inherent photocathode resolution must not be the limiting factor.

Take the following values

$$(s/n)^2 = 1000$$
$$T = .89$$
$$\Theta = 5\%$$
$$t_{.1} = 0.1 \text{ sec}$$
$$\sqrt{\frac{N}{t_1}} = 1.6 \times 10^3$$

Substituting then, one has

$$B\alpha^2 \quad D^2 = 1.92 \times 10^{-3}$$

Figure 26 shows the angle α and resulting lens diameter D plotted as a function of scene brightness. Several pertinent brightness levels are noted on the figure such as lunar night maximum.

At this point the camera system designer must determine the limits to "reasonable" aperture and resolution. Large optics pose problems in initial cost and fabrication. Mounting and steering equipment for a 100 cm lens or mirror is quite a bit larger and bulkier than for a 10 cm optic. An excellent analysis of vehicle structural constraints (Ref. 11) shows this clearly. The required resolution for surveillance will be generally specified by the field of view requirement. In some guidance and navigation systems for lunar vehicles (Ref. 12) rather high resolution requirements have emerged. This is particularly true in fully automatic navigation systems.

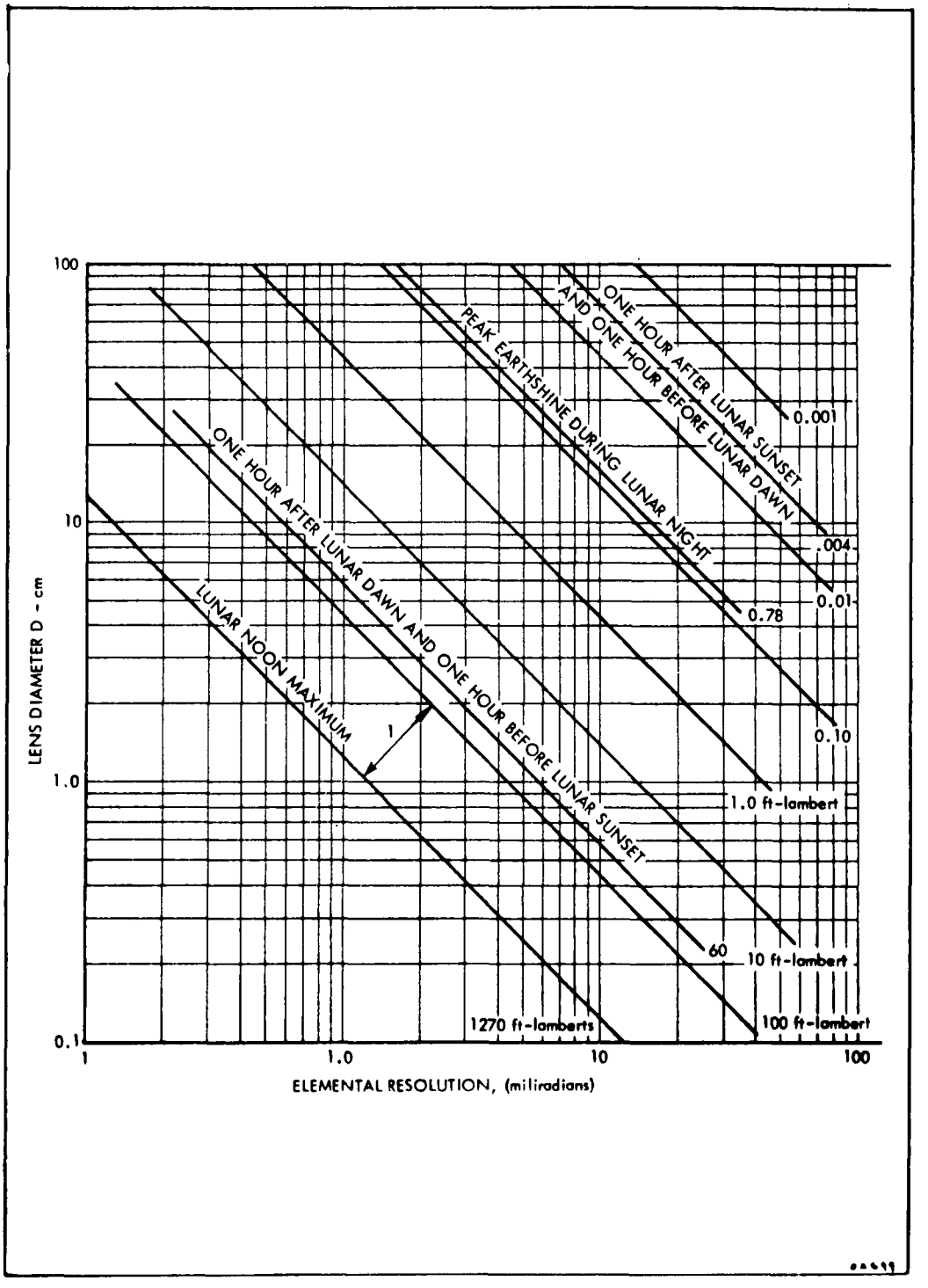

Figure 26. Relationship Between Elemental Resolution, Lens Diameter and Scene Brightness for Camera System where t_1 = 0.1 sec

It is instructive to examine Figure 27 closely. If other vehicle restraints limit the maximum lens aperture to 12.5 cm only those alternatives located below the line

$$12.5 \text{ cm} = \text{constant}$$

are available to the designer.
In the same way, if vehicle navigation requirements specify a resolution no poorer than 10 milliradians, only the alternatives to the left of the line

$$10 \text{ milliradians} = \text{constant}$$

are available.

The designer can now choose to cover the range of scene brightness levels within the allowed area by several means. Aperture can be varied, resolution can be varied, a neutral density filter may be inserted in front of the camera tube or a combination of these may be employed. Consider a case where only daytime operation is required—scene brightness will vary from 60 to 1270 foot lamberts. The designer might choose a constant resolution value, say, 1.0 milliradian, and vary the aperture from 1.25 to 5.7 cm. Or the aperture might be taken as fixed at 2 cm and the resolution would then vary from .6 to 2.9 milliradians. If it is desired to hold the variation in either parameter to some fixed ratio, as for example where the resolution will vary only from 1.0 to 2.0 milliradians, Figure 26 will show the required variation in the dependent parameter. This is shown as the line labeled (1).

For a 2/1 change in resolution then a change in aperture from 1.2 to 2.9 cm would be required. The effect of a neutral density filter can be easily evaluated by changing the scene brightness values by an appropriate factor. Night viewing would require extremely large lens apertures for the case shown where $t_1 = 0.1$ second. Figure 27 shows a second case where t_1 has been increased to 10 seconds. Note now that if limits on aperture and resolution are still taken to be 12.5 cm and 10 milliradians, lunar night viewing is now possible. It should be emphasized that considerable earthshine is available at the particular landing point chosen. The lines labeled sunset/sunrise in Figure 27 are equivalent to scene brightness levels for one hour before sunset and one hour after sunrise. It is of interest to calculate what would be required to view the lunar scene under conditions of starlight illumination only. This is shown in Figure 28. Starlight illumination was taken to be 9×10^{-5} foot candles and resultant scene brightness taken to be 9×10^{-6} foot lamberts. Examination of Figure 28 shows the inadvisability of attempting lunar night surveillance with a vidicon.

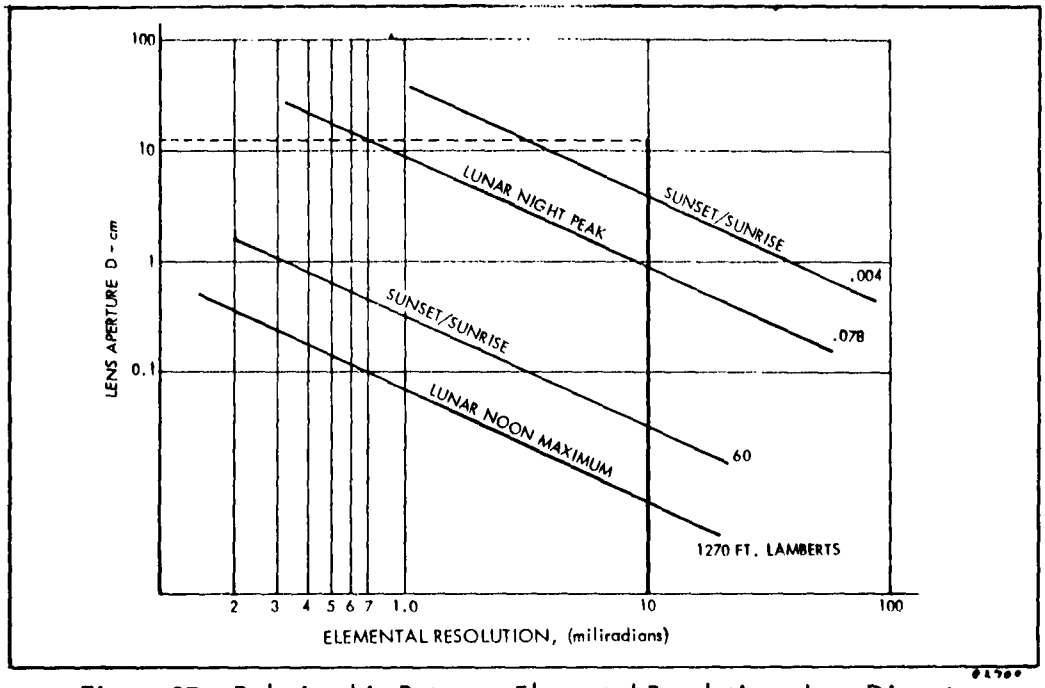

Figure 27. Relationship Between Elemental Resolution, Lens Diameter and Scene Brightness where t_1 = 10 sec

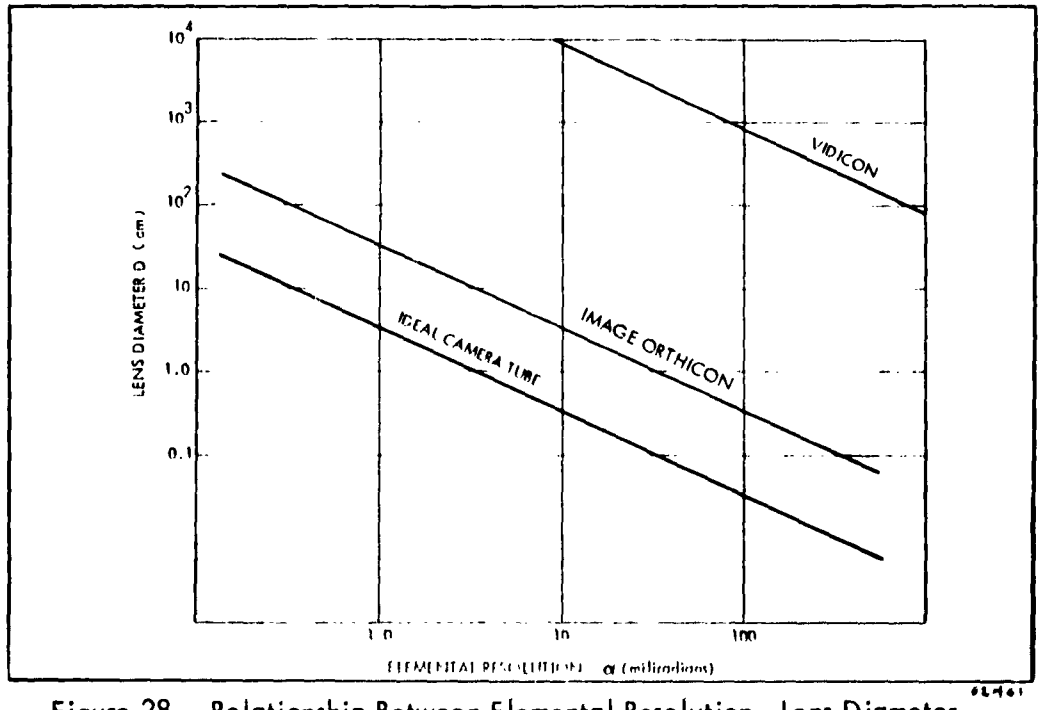

Figure 28. Relationship Between Elemental Resolution, Lens Diameter and Scene Brightness for t_1 = 10 sec Starlight Illumination Only

Lens apertures of thousands of centimeters would be required. Performance curves for an image orthicon ($n_q = 100$) and the ideal camera tube ($n_q = 1.0$) are included for comparison.

It should be noted that average scene brightness levels only have been discussed above. Scene reflectance was taken at 10%. The possibility then clearly exists where individual highlights within the scene may possess lighter reflectivity perhaps approaching 100% and therefore appear as much as ten times brighter. It is equally possible that scenes may be encountered where average reflectivity is less than 10%. Over-all system performance will of course be degraded then. The main effect of the variations in reflectivity within a given scene will be felt in the dynamic range requirements for the electronics.

Equation (6) holds for the case where exposure time and frame time are identical as in commercial television broadcasting. Television transmissions of this type are conceivable for lunar vehicles where real-time pictures are required regardless of the high cost in terms of transmitter power and equipment. Another mode is sometimes advantageous where exposure time and frame time are unequal. For example, as is beirg done for the Ranger program, the image is shuttered onto the cathode for milliseconds. Then this image is retained and read out at a greatly reduced rate of several seconds. This longer read-out time allows the use of narrower transmission bandwidth and reduced transmitter power. Equation (9) takes a different form in this case as shown below

$$B = \frac{2.8}{T} \quad \frac{(s/n)^2}{D^2 \alpha^2 \, t_1} \quad \frac{0.6}{\theta} \sqrt{\frac{N}{t_2}} \times 10^{-13} \text{ ft lamberts} \tag{10}$$

Where on must differentiate between t_1 and t_2

t_1 = exposure time

t_2 = one frame read-out time

Equation (10) shows that a system gains in sensitivity linearly with increasing exposure time and loses in sensitivity with the reciprocal of $\sqrt{t_2}$.

Let $t_2 = K_o^2 \; t_1$

Then equation (10) becomes

$$B = \frac{2.8}{\pi T} \; \frac{(s/n)^2}{D^2 \alpha^2 t_1} \; \frac{0.6}{\Theta} \sqrt{\frac{N_2}{K_o^2 \; t_1}} \times 10^{-13} \qquad (11)$$

or

$B = B_o \; \frac{1}{K_o}$ where B_o is equation (9)

This simple expression allows one to utilize all the preceding figures originally derived for the special case $t = t_1$. Division by the constant K_o is all that is required. As an example, suppose t_2 = 10 seconds, t_1 = 10 milliseconds, K_o^2 = 1000 and K = 33. Refer now to Figure 28. All lines of constant scene brightness must now be adjusted to a newvalue 33 times greater than that marked. In this case, exposure time has been shortened and sensitivity of the over-all camera system degraded. If t_1 had been held constant at 10 seconds and t_2 reduced to 1 second, K_o would be less than one, indicating that over-all sensitivity is decreased. This is intuitively obvious. Signal has been held constant but noise has been increased, due to wider bandwidth requirement.

The preceding discussion can be taken to apply to any lunar based surveillance system, mobile or permanently fixed. One might inquire then into the special problems posed by a mobile system. One of the first questions that arise is whether all or some pictures will be taken with the vehicle in motion. If all pictures are to be taken from a stationary vehicle considerable equipment simplification results.

If pictures are to be taken from a moving vehicle, the whole gamut of stabilization and tracking problems must be considered. It is not likely that this requirement will exist before the arrival of manned vehicle.

The lunar scene in general can be considered static. For the time scale envisioned for Surveyor or Prospector roving vehicles, no appreciable number of moving objects are anticipated on the lunar surface. The motion of the sun across the sky is comparatively sedate, 0.55 degrees/hour, and one would not expect profound changes in scene lighting over a period of one second. For daytime viewing shutter speeds (or exposure time) for the vidicon need only be milliseconds. Negligible blurring of the image would be expected. For nighttime viewing using earthshine, no problem is anticipated since the earth remains essentially fixed in the lunar sky. Still, one should not take the change in sun position lightly. With no lunar atmosphere, objects will leap from the extreme black of lunar shadows to full sunlight as the ascending sun illuminates them.

It is of interest to compute the rate of change of shadow length cast by a cliff onto a flat lunar plain as a function of sun elevation angle

Let x = height of cliff
l = shadow length
Θ = sun elevation angle

See Figure 29.

Given the following relationship

$$\tan\Theta = \frac{x}{l}$$

$$\frac{d}{dt}\left(\tan\Theta\right) = \frac{d}{dt}\left(\frac{x}{l}\right)$$

or

$$\sec^2\Theta \frac{d\Theta}{dt} = \frac{-x}{l^2} \frac{dl}{dt}$$

$$\frac{1}{\cos^2\Theta} \frac{d\Theta}{dt} = -\left(\frac{x}{l}\right)^2 \times \frac{dl}{dt}$$

Figure 29. Rate of Change of Shadow Length as a Function of Sun Elevation Angle

and

$$\frac{x}{\sin^2\Theta}\ \frac{d\Theta}{dt} = -\frac{dl}{dt}$$

now

$$\frac{d\Theta}{dt} = 0.55 \text{ degrees/hour}$$

and for this particular example

$$x = 1,000 \text{ ft}$$

$$\frac{-dl}{dt} = \frac{0.153}{\sin^2\Theta} \text{ ft/sec} \qquad (12)$$

Equation (12) is plotted in Figure 29. One can see that navigation and general surveillance may be hampered somewhat during the hours preceeding the sunset and following the dawn.

In summation, operation of a vidicon surveillance system during the lunar day poses no more conceptual problems than analogous terrestial day operation. Operation is feasible during the lunar night in areas where earthshine is appreciable. Shutter times of several seconds can be utilized in conjunction with long read-out times to provide useful television coverage. In lunar areas where only starlight illumination is available, an additional source of light must be provided for the vidicon.

REFERENCES

1. Kosyrev, N. A. Luminescence of the Lunar Surface and Intensity of Corpuscular Radiation from Sun. Publ. Crimean Astrophys, Obs., 16, 148-158. 1956.

2. Barabasheff, N. Polarimetrische Beobachtungen und der Mondoberflache und an Gesteinen. A. N. 229, 9-14, 1927.

3. Wright, F. E. Polarization of Light Reflected from Rough Surfaces with Special Reference to the Light Reflected by the Moon. Proc. Nat. Acad. Sci., 13, 535-540, 1927.

4. Dolfus, A. La Courbe de Polarisation de la Terre et la Nature du Sol Lunaire. C. R., 235, 1013-1016.

5. Buwalda, P. The Lunar Environment. (TR 34-159 NASA Contract No. NASw-6) Pasadena, Calif.: Jet Propulsion Laboratory, California Institute of Technology, 28 October 1960.

6. Final Report, Norden-Ketay Corp., Report No. 152120001, Contract No. AF 18(600)-1746.

7. Russell, H. N. "Stellar Magnetudes of the Sun, Moon and Planets," Astrophysical Journal, Vol. 43, pp 173-196. 1961.

8. Space Programs Summary No. 37-9, Vol. 1. Pasadena, Calif.: Jet Propulsion Laboratory, California Institute of Technology. Pages 20-24, 1 March 1961-1 May 1961.

9. Rose, A. The Relative Sensitivities of Television Pickup Tubes, Photographic Film, and the Human Eye. Proc. IRE, 30(6): 293 (June 1942).

10. Rose, A. A Unified Approach to the Performance of Photographic Film, Television Pickup Tubes, and the Human Eye. J. Society of Motion Picture Engineers 47: 273 (October 1946).

11. Myton, M. "Analysis of Effects of Structural Constraints on Vignetting of Camera Telescopes for a Class of Lunar Vehicles Characterized by Stereo, Color Camera Systems." Santa Barbara, Calif.: G. E. Space Systems Operation.